International Journal of Innovative Technology and Exploring Engineering (IJITEE)
ISSN: 2278-3075 (Online), Volume-8 Issue-11, September 2019

Variable Parameter Resized Zero Attracting Least Mean Fourth Control for Grid-Tied PV System

Md. Ibrahim, M.A. Mallick, Mukul Chankaya, Atif Iqbal, Ikhlaq Hussain

Abstract: ***This paper presents the variable parameter resized zero attracting least mean fourth (VP-RZA-LMF) control algorithm for grid-tied photovoltaic (PV) system. The proposed control algorithm is superior over the conventional control algorithms in terms of swift response and handling the irregular nature of solar irradiations. The DC bus voltage control is incorporated in voltage source converter (VSC) control. The boost converter utilizes the maximum power point tracking (MPPT) algorithm for producing its gating sequence to keep PV array voltage constant.***

Keywords—Photovoltaic (PV), grid-tied, variable parameter resized zero attracting least mean square (VP-RZA-LMS)

I. INTRODUCTION

The modern power system is facing new challenges day by day, with the rapidly growing demand for power. The fossil fuel-based power generation has been adding up to environmental concerns like increasing carbon footprint and green-house gases emissions. which cause global warming, acid rain, and depletion of the ozone layer [1]. It is necessary to induct new power generation sources along with coal operating the power plant due to depleting fossil fuel reserves. The solar thermal, Photovoltaic (PV), tidal, wind, and biomass are few of the matured renewable power generation technologies. The PV systems are gaining popularity [2] over other non-conventional power generation resources due to its simple operation and ease of installation unlike solar thermal, wind and geothermal plants. The PV system can penetrate the conventional grid at almost any scale ranging from few kW rooftop plants to 10's of MW ultra mega PV plants [3]. With technological advancements, the cost of the PV system has become very affordable to individuals, unlike thermal solar and wind power plants that need huge investment and special skills to install. Countries like the US, China and India [4] are leading the world in promoting the PV system as a viable option for providing the required power. The PV system with a conventional grid can overall reduce carbon footprint along with the greenhouse gasses emission. The PV system may be integrated into the grid via a single-stage or dual-stage topology. In single-stage topology, the PV system is directly connected to DC bus, whereas, in dual-stage boost, the converter is utilized in between PV and voltage source converter (VSC) [5].

Manuscript published on 30 September 2019.
*Correspondence Author(s)
Md. Ibrahim, Electrical Engineering Department, Integral University, Lucknow, India. ibrahimalig3893@gmail.com
Mukul Chankaya, Electrical Engineering Department, Kashmir University, Srinagar, India. mukulchankaya@gmail.com
Ikhlaq Hussain Electrical Engineering Department Kashmir University, Srinagar, India. ikhlaqiitd2015@gmail.com
M.A. Mallick, Electrical Engineering Department, Integral University, Lucknow, India. mamallick@iul.ac.in
Atif Iqbal, Electrical Engineering Department, Qatar University, Qatar. atif2004@gmail.com

The dual-stage topology of grid integration is beneficial and efficient for a system having DC voltage (V_{DC}) < 750 V. Many maximum power point tracking (MPPT) algorithms are mentioned in the literature to extract maximum power from the PV system [6]. Due to variation in irradiation level and ambient temperature the operating point keeps on changing from maximum power point (MPP).

Several VSC control has been mentioned in literature and can be categorized in terms of conventional, adaptive and intelligent controls i.e. unit template, synchronous reference frame (SRF), Least mean fourth (LMF), direct power control, discrete Fourier transform, droop control and artificial intelligence (AI) based technique[7]. Which are unilized to mitigate the power quality problems.

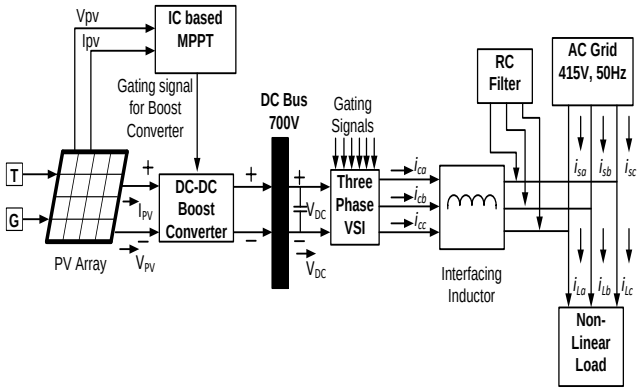

Fig. 1. Block diagram of the proposed topology

The proposed system presents a 3-phase 3-wire grid-tied dual stage PV System [8] simulated in MATLAB/SIMULINK environment. The controls are provided for boost converter and VSC. The main contributions of the proposed system are

a. The dual-stage PV system provides constant DC link voltage irrespective of irradiation and temperature variation.
b. The VSC perform a multi-functional operation for mitigating power quality issues
c. The VSC control is provided by a variable parameter re-sized zero attracting least mean fourth (VP-RZA-LMF) [9] algorithm for its better and faster response due to less mean square error (MSE).

II. PROPOSED TOPOLOGY

The proposed system is shown in Fig.1. The PV system of 32 kW is connected to DC bus via boost converter[10]. The control signal of the boost converter is generated from the duty cycle provided by MPPT based on incremental conductance (IC) method. The V_{DC} is maintained constant across VSC with the help of the capacitor.

The VSC perform the harmonics suppression, load balancing and voltage regulation with the proper switching sequence at the point of common coupling (PCC). The interfacing inductance (L_{int}) and RC filter are utilized for eliminating the voltage and current ripples generated by the non-linear load.

III. CONTROL STRATEGY

The proposed control scheme is consist of MPPT and VSC control. The VSC control is shown in Fig.2. The VP-RZA-LMF is an adaptive control algorithm that reduces the excess mean square error (EMSE) by varying the size of the parameter in each iteration.

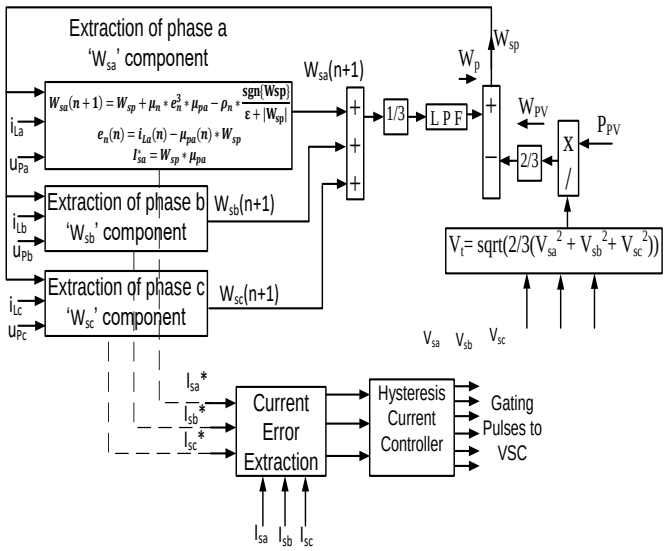

Fig.2. Voltage source converter

A. MPPT Control

The MPPT based on IC algorithm senses the instantaneous PV voltage (V_{PV}) and PV current (I_{PV}). The (1),(2) & (3) govern the IC algorithm are described below. Where 'e' is the error tolerance which ideally should be zero and D is the duty cycle[11].

$$dI_{PV}/dV_{PV} + I_{PV}/V_{PV} = e; \text{ at MPP; D optimized} \quad (1)$$

$$dI_{PV}/dV_{PV} + I_{PV}/V_{PV} > e; \text{ D increases} \quad (2)$$

$$dI_{PV}/dV_{PV} + I_{PV}/V_{PV} < e; \text{ D decreases} \quad (3)$$

The D is further compared with the triangular signal of 10 kHz to provide the gating signals for the boost converter. Which maintains the (V_{PV}) constant irrespective of irradiation and ambient temperature variation.

B. VSC Control

VSC control is shown in Fig. 2. The error (e_n) is calculated as per (4), where the load current of phase 'a' (i_{La}), the unit template of phase 'a' (μ_{pa}) and feedback weight component (W_{sp}) as per (10) of the proposed control are utilized. The feed forward term of the PV system (W_{PV}) is calculated as per (5), using the sensed phase voltages of the source (V_{sa}, V_{sb} & V_{sc}) and power supplied by the PV system (P_{PV}). The extracted weight component of each phase (W_{sa}, W_{sb} & W_{sc}) are calculated [12] as per (6),(7) & (8), where μ_n is the positive step size chosen for stabilizing the system, ρ_n is the shrinkage parameter and ε is the scaling factor. The average weight component (W_p) is calculated as per (9). The reference current signals ($I^*_{sa}, I^*_{sb}, I^*_{sc}$) are calculated as per (11) and further negated with sensed source currents of each phase (I_{sa}, I_{sb}, I_{sc}) to generate the VSC gating pulses utilizing hysteresis current controller.

$$e_n = i_{La} - \mu_{pa} * W_{sp} \quad (4)$$

$$W_{PV} = \frac{2}{3}\left(\frac{P_{PV}}{\sqrt{\frac{2}{3}(V_{sa}^2+V_{sb}^2+V_{sc}^2)}}\right) \quad (5)$$

$$W_{sa}(n+1) = W_{sp} + \mu_n * e_n^3 * \mu_{pa} - \rho_n * \frac{sgn\{Wsp\}}{\varepsilon+|W_{sp}|} \quad (6)$$

$$W_{sb}(n+1) = W_{sp} + \mu_n * e_n^3 * \mu_{pb} - \rho_n * \frac{sgn\{Wsp\}}{\varepsilon+|W_{sp}|} \quad (7)$$

$$W_{sc}(n+1) = W_{sp} + \mu_n * e_n^3 * \mu_{pc} - \rho_n * \frac{sgn\{Wsp\}}{\varepsilon+|W_{sp}|} \quad (8)$$

$$W_p = 1/3\,(W_{sa} + W_{sb} + W_{sc}) \quad (9)$$

$$W_{sp} = W_p - W_{pv} \quad (10)$$

$$I^*_{sa} = W_{sp} * \mu_{pa};\ I^*_{sb} = W_{sp} * \mu_{pb};\ I^*_{sc} = W_{sp} * \mu_{pc} \quad (11)$$

C. Selection of DC bus voltage and capacitor

The V_{DC} are calculated as per (12).

$$V_{DC} = 2\sqrt{2} * V_{LL}/\sqrt{3} * m \quad (12)$$

Where m is the modulating index considered as unity (m=1) and V_{LL} is the source line voltage. DC bus capacitor C_{DC} can be calculated as per (13w).

$$\frac{1}{2}C_{DC}(V_{DC}^2 - V_{DC1}^2) = 3K_1 * V_{sa} * a * I * t \quad (13)$$

Where V_{DC} is the nominal voltage, V_{DC1} is the minimum voltage level, 'a' is overloading factor, 'V_{sa}' is the phase voltage and 't' is the time within which V_{DC} should be recovered[13].

IV. SYSTEM PERFORMANCE

The proposed system has 32 kW of PV system incorporated. The PV power (P_{PV}) is supplied to the grid via boost converter. The non-linear load of 15.5 kW is simulated at the load end. The source voltage is 415 V (rms) at 50 Hz. The system is operated under steady-state and dynamic state i.e. varying insolation and load unbalancing conditions.

A. Steady-State Performance

During steady-state operation, the solar insolation level is kept at 1000 W/m^2 and temperature at 25°celsius. The total harmonics distortion (THD) of source voltage, source current and load current are shown in Fig. 3(a),(b) & (c), which are satisfactory as per IEEE 519 standards. The source voltage(V_{sabc}), source current (i_{sabc}), load current of phase 'a' (i_{La}) compensator current of phase 'a' (i_{Ca}), active and reactive power supplied to the grid (P_g & Q_g) are shown in Fig. 4 (a). The V_{PV}, I_{PV}, P_{PV} & V_{DC} are shown in Fig.4 (b).

Retrieval Number: K18690981119/19©BEIESP
DOI: 10.35940/ijitee.K1869.0981119
Journal Website: www.ijitee.org

Published By:
Blue Eyes Intelligence Engineering and Sciences Publication (BEIESP)

The presented system maintains the unity power factor (UPF) throughout the operation. The V_{DC} is maintained at 700 V. The P_g supplied to the grid is around 15 kW and Q_g is zero during steady-state operation.

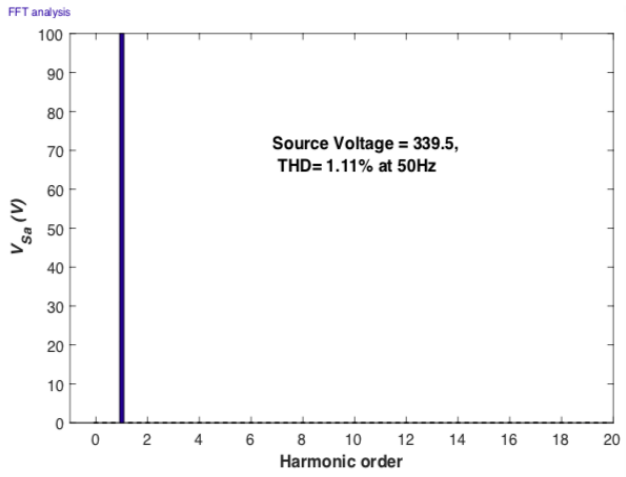

(a)

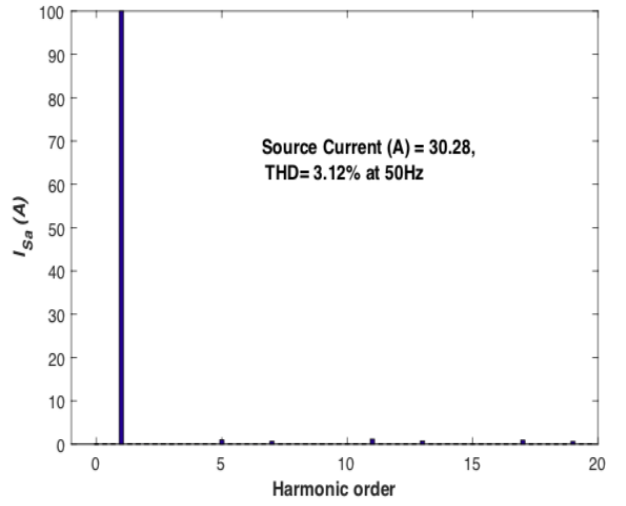

(b)

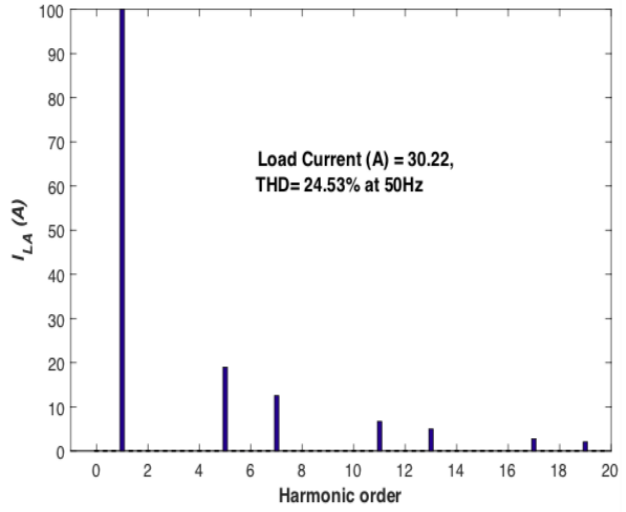

(c)

Figs.3.(a),(b) & (c) Harmonic content of (a) i_{sa} (b) v_{sa} and (c) i_{La} during steady-state

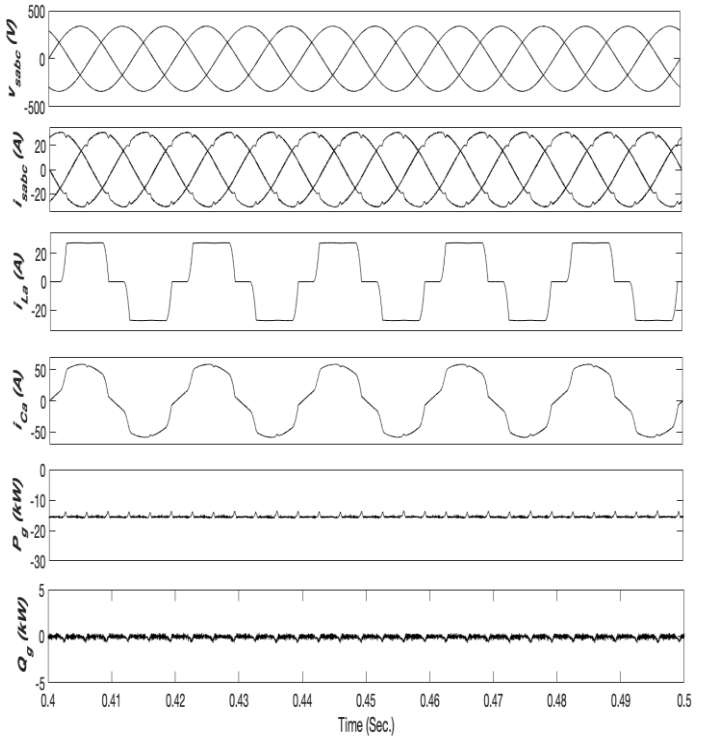

(a)

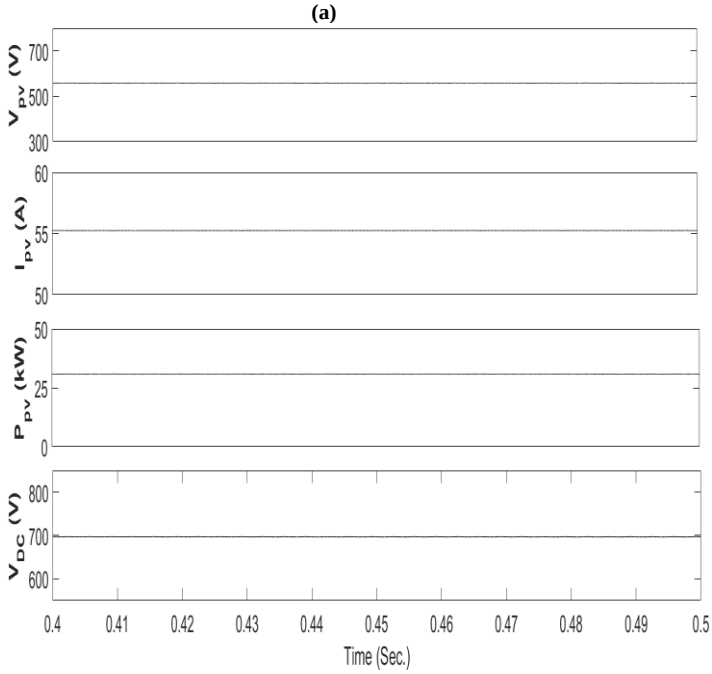

(b)

Figs 4. Steady-state performance of (a) v_{sabc} i_{sabc}, i_{La}, i_{Ca}, P_g & Q_g (b) V_{PV}, I_{PV}, P_{PV} & V_{dc}

B. Dynamic-State Performance with Varying Irradiation

During dynamic-state operation the solar irradiation level changes from 600 $^{W}/_{m^2}$ to 1000 $^{W}/_{m^2}$ at 0.6 sec of simulation time. The P_g changes from few hundred watts to 15 kW as irradiation level increases. The system maintains the UPF between v_{sabc} & i_{sabc} while maintaining the Q_g at zero as shown in Fig. 5(a). The V_{PV} & V_{dc} are maintained at the same state as in steady-state operation.

Retrieval Number: K18690981119/19©BEIESP
DOI: 10.35940/ijitee.K1869.0981119
Journal Website: www.ijitee.org

Published By:
Blue Eyes Intelligence Engineering and Sciences Publication (BEIESP)

The corresponding change in I_{PV} & V_{PV} are shown in Fig. 5(b).

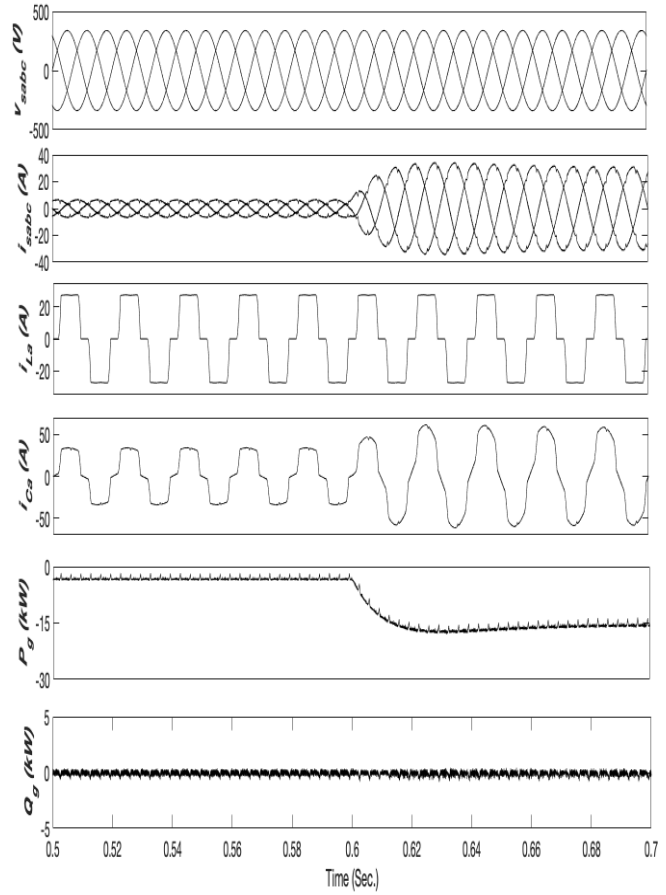

(a)

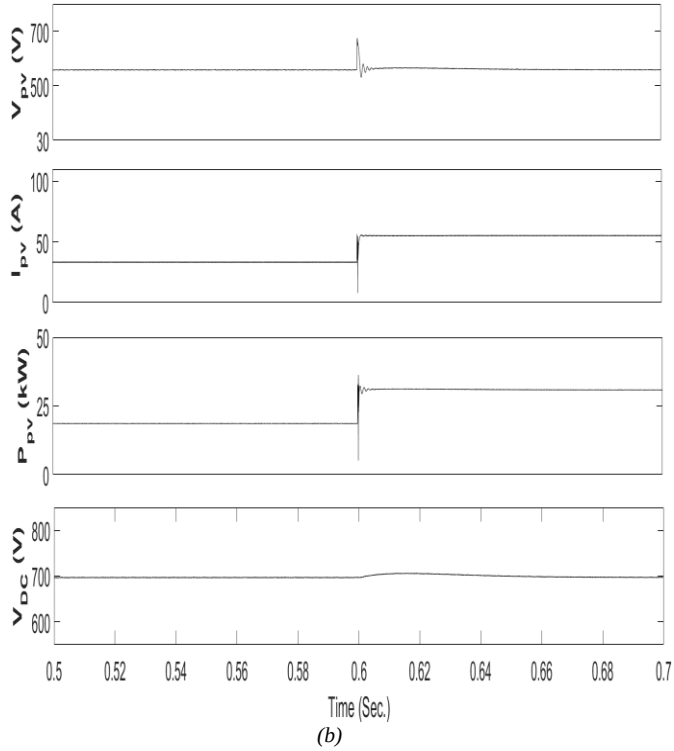

(b)

Figs. 5. Dynamic-state performance under varying solar irradiations of (a) v_{sabc} i_{sabc}, i_{La}, i_{Ca}, P_g & Q_g (b) V_{PV}, I_{PV}, P_{PV} & V_{dc}

C. *Dynamic-State Performance under Load Unbalancing*

During dynamic-state operation load of phase 'a' is detached from the grid to create the load unbalancing. The i_{La} remains zero till 0.5 sec of the simulated time and then returns to balanced load condition as shown in Fig. 6 (a). During which the VSC provides the i_{Ca} to maintain the balance of the system. The unbalancing has no effect on the DC side of the system as V_{PV}, I_{PV}, P_{PV} & V_{dc} maintains the same state as in steady-state operation as shown in Fig. 6 (b). The weight components of the corresponding unbalanced system are shown in Fig. 7. Where the change in W_p, W_{sp} are noticeable from unbalanced to balanced load.

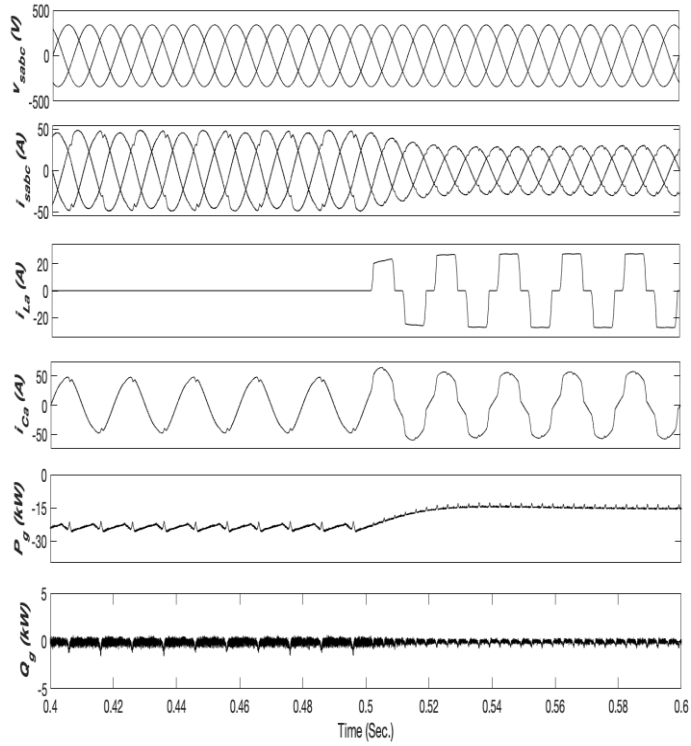

(a)

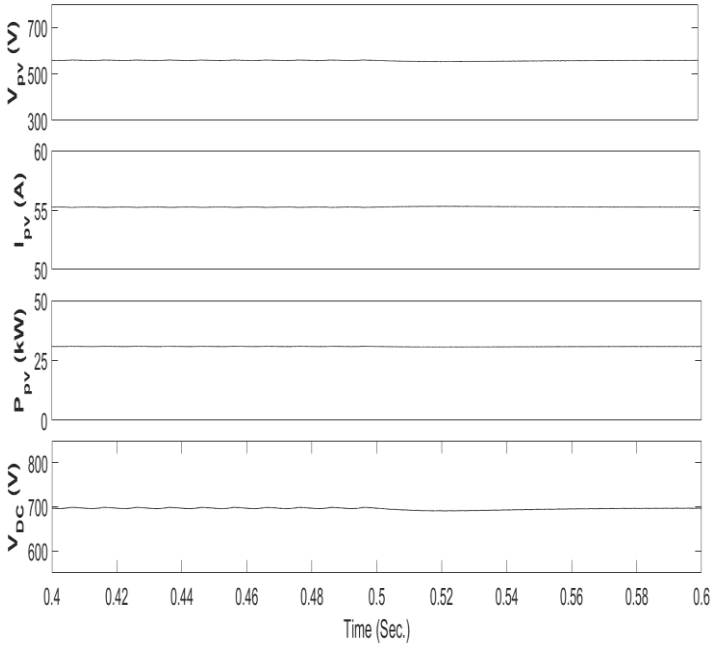

(b)

Figs.6. Dynamic-state performance under load unbalancing of (a) v_{sabc} i_{sabc}, i_{La}, i_{Ca}, P_g & Q_g (b) V_{PV}, I_{PV}, P_{PV} & V_{dc}

Retrieval Number: K18690981119/19©BEIESP
DOI: 10.35940/ijitee.K1869.0981119
Journal Website: www.ijitee.org

Published By:
Blue Eyes Intelligence Engineering and Sciences Publication (BEIESP)

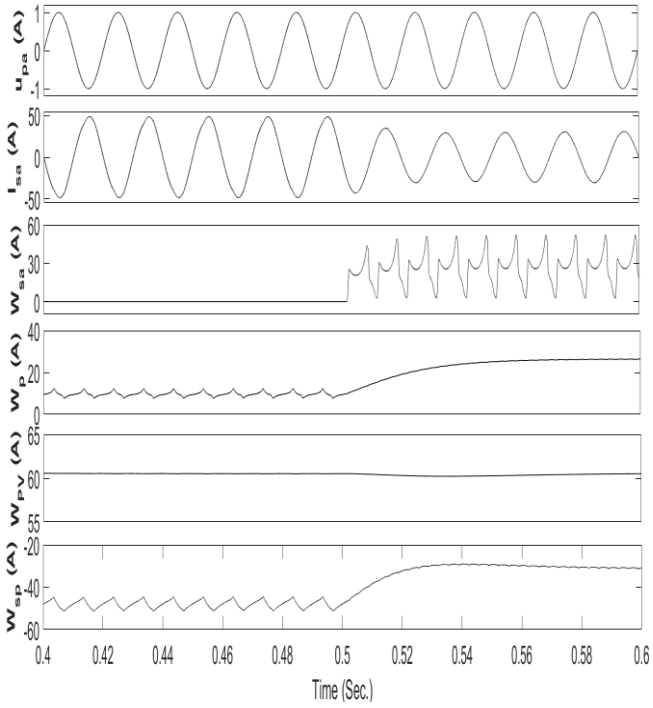

Fig.7. Dynamic-state performance under load unbalancing of μ_{pa}, I_{sa}, W_{sa}, W_P, W_{PV} & W_{sp}

V. CONCLUSION

The 3-phase 3-wire grid-tied PV system with VP-RZA-LMF adaptive control algorithm has been proposed. The system performance has been analyzed under steady-state and dynamic-state conditions. The v_{sabc}, i_{sabc} are in phase opposition as power is being transferred to the grid from the PV system while maintaining the UPF. The THD of the presented system during steady-state has been well below 5% and accepted as per IEEE 519 standards. The system behavior is found satisfactory under varying irradiation and load unbalancing conditions. The exchange of Q_g of grid and PV system is kept zero throughout the operation.

VI. ACKNOWLEDGMENT

I am very thankful to Prof. Mohd. Arifuddin Mallick ,Dr Ikhlaq Hussain and Mr Mukul Chankaya for inspiring me to model and simulate it as simulation on MATLAB/Simulink. I am thankful to Integral University for registering my manuscript MCN: IU/R&D/2019-MCN 000706.

APPENDIX

System Parameters: The PV module voltage, V_{mpp}=26.3 V; PV module current, I_{mpp}=7.614 A; no. of parallel module, n_p =7; no. of series module, n_s =23; PV array voltage, V_{pv}=605 V; PV array current, I_{pv}=53.29 V; PV array power, P_{pv}=32 kW; boost inductor, L_b=3.11 mH; DC link capacitor, C_{dc}= 10000 µF; DC link voltage PI control, K_{Pdc}= 1 and K_{idc} =0; V_{dc} =700 V; VSC = 35 kVA; adaptive filter constant, μ_n =0.01, ρ_n =0.006 & ε =0.002; interfacing inductance, L_{int}=4 mH; 3-phase grid voltage, V_{sabc}= 415 V (rms); RC filter, R_f=10 Ω and C_f=10 µF; 3-phase non-linear load = 15.5 kW, sampling time, T_s= 10 µs.

REFERENCES

1. U. Aswathanarayana, *Solar energy*. Elsevier Inc., 2010.
2. E. Kabir, P. Kumar, S. Kumar, A. A. Adelodun, and K. H. Kim, "Solar energy: Potential and future prospects," *Renew. Sustain. Energy Rev.*, vol. 82, no. September 2017, pp. 894–900, 2018.
3. M. Rathbun, Y. Xu, R. R. nejad, Z. Qu, and W. Sun, "Impact Studies and Cooperative Voltage Control for High PV Penetration," *IFAC-PapersOnLine*, vol. 51, no. 28, pp. 684–689, 2018.
4. V. A. Suryad, S. Doolla, and M. Chandorkar, "Microgrids in India: Possibilities and challenges," *IEEE Electrif. Mag.*, vol. 5, no. 2, pp. 47–55, 2017.
5. A. K. Singh, I. Hussain, and B. Singh, "Double-Stage Three-Phase Grid-Integrated Solar PV System With Fast Zero Attracting Normalized Least Mean Fourth Based Adaptive Control," *IEEE Trans. Ind. Electron.*, vol. 65, no. 5, pp. 3921–3931, 2018.
6. N. Karami, N. Moubayed, and R. Outbib, "General review and classification of different MPPT Techniques," *Renew. Sustain. Energy Rev.*, vol. 68, no. September 2016, pp. 1–18, 2017.
7. N. Beniwal, I. Hussain, and B. Singh, "Hybrid VSS–LMS–LMF based adaptive control of SPV-DSTATCOM system under distorted grid conditions," *IET Renew. Power Gener.*, vol. 12, no. 3, pp. 311–322, 2017.
8. N. Saxena, B. Singh, and A. L. Vyas, "Integration of solar photovoltaic with battery to single-phase grid," *IET Gener. Transm. Distrib.*, vol. 11, no. 8, pp. 2003–2012, 2017.
9. D. Jin, J. Chen, C. Richard, and J. Chen, "Model-driven online parameter adjustment for zero-attracting LMS R," *Signal Processing*, vol. 152, pp. 373–383, 2018.
10. A. Nicastri and A. Nagliero, "Comparison and evaluation of the PLL techniques for the design of the grid-connected inverter systems," *IEEE Int. Symp. Ind. Electron.*, pp. 3865–3870, 2010.
11. N. Saxena, I. Hussain, B. Singh, and A. L. Vyas, "Implementation of a Grid-Integrated PV-Battery System for Residential and Electrical Vehicle Applications," *IEEE Trans. Ind. Electron.*, vol. 65, no. 8, pp. 6592–6601, 2018.
12. M. Jiang, W. Liu, and Y. Li, "Adaptive Beamforming for Vector-Sensor Arrays Based on a Reweighted Zero-Attracting Quaternion-Valued LMS Algorithm," *IEEE Trans. Circuits Syst. II Express Briefs*, vol. 63, no. 3, pp. 274–278, 2016.
13. B. Singh, A. Chandra, and K. Al-haddad, *Power Quality Problems and Mitigation Techniques - Wiley Online Library*.